

OPTIMIZATION OF ACID HYDROLYSIS PROCESS PARAMETERS FOR OBTAINING CRYSTALLINE NANOCELLULOSE: HIGHER CRYSTALLINITY AND LOWER ASPECT RATIO

MURTAZA HAIDER SYED,* KHODIJAH AL QUBRO,** NORHAYATI ABDULLAH* and MIOR AHMAD KHUSHAIRI MOHD ZAHARI*

*Faculty of Chemical and Process Engineering Technology, Universiti Malaysia Pahang Al-Sultan Abdullah, Gambang, Pahang, Malaysia

**Faculty of Engineering, Universitas Indo Global Mandiri, Jalan Jendral Sudirman No. 629, Palembang, South Sumatera, Indonesia

✉ Corresponding authors: M. H. Syed, murtazahaidersyed@gmail.com
M. A. K. Mohd Zahari, ahmadkhushairi@umpsa.edu.my

Received September 4, 2025

Cellulose is the most abundant renewable biopolymer on Earth. Due to its special properties, it is widely used and studied. Nano-sized cellulose, and specifically cellulose nanocrystals (CNCs), have great potential for biomedical applications. Although many studies have been published on obtaining CNCs from various sources and by different methods, to the authors' knowledge, the current literature focuses mainly on the yield % of CNCs, lacking optimization for obtaining higher crystallinity. Considering that crystallinity and aspect ratio are extremely important in biomedical applications, the present study optimized four major parameters: acid type, acid percentage, duration of acid treatment, and temperature of the acid hydrolysis process. The developed CNCs were characterized using FTIR and XRD. Crystallinity index was measured for each parameter in order to find the optimum parameters for maximum crystallinity. Finally, TEM analysis was used to determine the aspect ratio of the CNC obtained under optimized conditions. Thus, the study obtained CNCs with higher crystallinity and a low aspect ratio (12.07). The findings can be used for industrial and lab applications to obtain CNCs for biomedical applications.

Keywords: crystalline nanocellulose, microcrystalline cellulose, acid hydrolysis, crystallinity

INTRODUCTION

The most prevalent natural biopolymer on Earth is cellulose, which is renewable, biodegradable, and non-toxic. With three hydroxyl groups for each anhydro glucose unit (AGU), cellulose has high functionality and degree of modification.^{1,2} Research on cellulose's mechanical, biological, and chemical characteristics has been extensive due to its applications in various sectors, including the biomedical one.^{3,4}

A novel family of nano-materials, cellulose nanocrystals (CNCs), has appeared as one of the most important nano forms of cellulose.⁵ CNCs have several advantages over cellulose fibres, including nanoscale size, high specific strength and modulus, large surface area, antimicrobial activity, and distinctive optical characteristics.⁶ Due to their remarkable physicochemical features and potential

uses, CNCs have attracted much research interest. Due to their biocompatibility, CNCs have gained much attention in biomedical applications, for example, in drug delivery,⁷ in the past decade. Their morphology and high anionic charge have been demonstrated to serve as significant advantages in sustained drug release.^{8,9}

There are numerous sources from which CNCs can be synthesized, including microcrystalline cellulose,¹⁰ bacterial cellulose,¹¹ cotton,¹² hardwood¹³ and softwood.¹⁴ Their major features include a large surface area (150 m²/g), an excellent aspect ratio (70), and a high tensile strength (7,500 MPa).¹⁵ However, the main quality required for biological applications is the crystallinity of CNCs. Much of the literature focuses on CNC yield percentage; however,

morphology has a crucial role if the aim is biomedical application.^{16,17}

Numerous CNC preparation techniques have been developed for different uses, including steam explosion, high pressure homogenization, ultrasonic technology, acid-/alkaline hydrolysis, enzyme-assisted hydrolysis, and combined procedures.^{18,19} Among them, acid hydrolysis is a widely recognized synthesis method with demonstrated efficiency. The main parameters (acid used, acid percentage, treatment duration, and temperature) can help control the crystallinity of the obtained CNCs.^{20,21}

A previous study²² reported the production of CNCs using phosphotungstic acid hydrolysis of microcrystalline cellulose. The study focused on the yield and characterization of CNCs; however, the effects of major parameters on the morphology of CNCs was not covered. In another study,²³ CNCs were obtained from date palm microcrystalline cellulose. The study focused on the conversion process and the characterization of CNCs. However, the study did not assess the effect of different treatment parameters on crystallinity. In general, in the literature, a comprehensive study that would cover the effects of all four main parameters to produce CNCs using acid hydrolysis, with a focus on crystallinity, is missing. In biomedical applications, crystallinity is a significant aspect, ensuring for example, accurate drug delivery, compared to amorphous materials, with a disorganized arrangement of atoms.²⁵ Therefore, the current study aims to address this gap, by optimizing all main parameters of acid hydrolysis of MCC to achieve higher crystallinity CNCs with a low aspect ratio.

EXPERIMENTAL

Chemicals

All the chemicals, including sulphuric acid (>99.8%), nitric acid (70%), hydrochloric acid (R&D), microcrystalline cellulose (R&D), as well as dialysis tubing (molecular weight cut-off = 14,000), were purchased from Sigma-Aldrich.

Cellulose nanocrystals synthesis

CNCs were prepared by acid hydrolysis of microcrystalline cellulose (MCC). Four major parameters control the output of the process, including the type of acid, percentage of acid, temperature, and duration of acid treatment. The four parameters were optimized to obtain CNCs with the highest crystallinity.²⁴

The acid type was selected by suspending microcrystalline cellulose in 32% of various acids, including H₂SO₄, HCl, and HNO₃, with distilled water in the solid to liquid ratio of 1:75. The suspensions were stirred at 500 rpm at 50 °C for 3.5 h. After cooling, the suspension was centrifuged at 5000 rpm using an Eppendorf Centrifuge 5810-R, and then dialysed against distilled water to remove excess acid until a neutral pH was achieved (measured continuously with a Mettler Toledo). Ultimately, the slurry was freeze-dried using a Christ/Alpha 2-4 LDplus to obtain CNCs.²⁰

Then, considering that H₂SO₄ was found the most efficient, the optimum acid percentage was determined by dissolving MCC in 28, 30, 32, 34, and 36% of H₂SO₄ at 50 °C for 3.5 h to obtain CNCs. The most efficient temperature was investigated by varying temperatures at 45, 50, 55, and 60 °C for 3.5 h. The effect of the duration of the acid hydrolysis treatment was determined by varying the treatment time as follows: 2, 2.5, 3, 3.5, and 4 h at 50 °C.

Characterizations

TEM microscopy is considered an essential tool for the detailed visualization of the crystal boundaries. The morphology of the produced CNCs was observed through TEM (JEM 1400, JEOL, Peabody, MA, USA), operated at an accelerating voltage of 100 kV. A 0.02% (w/v) CNC suspension in distilled water was formed. The suspensions were deposited on carbon-coated TEM grids. After the samples were completely dried, the images were taken for TEM analysis. The dimensions of the CNCs were calculated using Image-J software (n=2) (National Institutes of Health, USA), while the distribution curves for dimensions were drawn using OriginPro 2022.

FTIR spectroscopy was performed using a Thermo Scientific Nicolet IS50 FTIR spectrometer using ATR crystals. The diamond window was cleaned first with ethanol to remove any impurities and disturbance during the scanning. After cleaning, the sample was placed on the diamond window and pressed against it using mechanical force. The results were recorded in the region from 4000 to 400 cm⁻¹ (32 scans and 4 cm⁻¹ resolution). After recording the spectra, they were further analyzed using Nicolet OMNIC software, and the graphs were drawn using OriginPro 2022.

The samples were directly measured (without any prior treatment) using an X-ray diffractometer (PANalytical X'pert Powder X-Ray Diffractometer, Cu anode) using a single-crystal silicon holder, fixed slit of 0.2177, Beta filter Ni (9430-031-51031), and LynxEye XE detector. The scanning was conducted over a range of 5°-80° at 1° min⁻¹ with a sampling step of 0.02° at room temperature. The data was then analyzed using HighScore Plus software, and the graphs were drawn using OriginPro 2022 software. The crystallinity index (CrI) was calculated using Segal's method:

$$CrI = \frac{I_{002} - I_{amorph}}{I_{002}} \quad (1)$$

where I_{002} represents maximum intensity, while I_{amorph} represents the intensity of $2\theta = 18^\circ$.²² The data manipulation including background subtraction and smoothing done using OriginPro 2022.

RESULTS AND DISCUSSION

FTIR analysis was performed to confirm the presence of specific functional groups and ultimately confirm the structure of the CNCs. XRD analysis was used to determine the crystallinity of the synthesized CNCs.

Effect of the acid

The acid used in CNC preparation can have significant effects on their crystallinity. In the current study, the acids examined for the acid hydrolysis of MCC to produce CNCs were: H_2SO_4 , HCl, and HNO_3 . The acid producing the CNCs with the highest crystallinity was further used to optimize the other parameters.

The FTIR analysis of the various CNCs produced by different acids is shown in Figure 1. The FTIR spectra of MCC showed the characteristic bands of the OH and C-H stretching vibrations, indicated by the band at 3340 cm^{-1} , as reported previously and confirmed from literature.²⁶ The band around 1650 cm^{-1} indicated the OH vibrations due to absorbed water, that at 1350 cm^{-1} indicated the C-H and C-O vibrations in the polysaccharide rings of cellulose, while the

band at 1060 cm^{-1} indicated the presence of C-O-C in the pyranose ring, as similarly reported previously.²⁷ The FTIR spectra of CNCs mainly showed similar bands to those of MCC, meaning there is no chemical modification in the CNCs. However, an additional band at 2350 cm^{-1} was observed in the CNCs after the acid treatment, indicating thiol and nitrile groups.²⁸ During the acid treatment with HCl, H_2SO_4 and HNO_3 , the interaction of chloride, sulphate, and nitrate ions with the hydroxy groups of the CNCs may have taken place.²⁰

The XRD patterns of CNC and MCC (Fig. 2a) both showed the characteristic bands at 15° , 22.5° , and 34.5° , consistent with the planes of (1-10), (200) and (004), corresponding to the presence of cellulose I, as confirmed in previous work.²⁹ However, the acid treatments differently affect the crystallinity of the CNCs, as shown by the crystallinity index (CrI) (Fig. 2b). Among the acids, the HCl treatment showed the minimum effect on crystallinity index (55.3%), and the HNO_3 treatment led to 60.8% crystallinity index. The maximum crystallinity of 65% was achieved by the H_2SO_4 treated MCC. Hydrochloric acid led to the minimum crystallinity (55%) as it failed to remove the amorphous regions of the MCC. The main reason for this is that the single proton of HCl, which makes it less effective than sulphuric acid, which has a diproton effect.

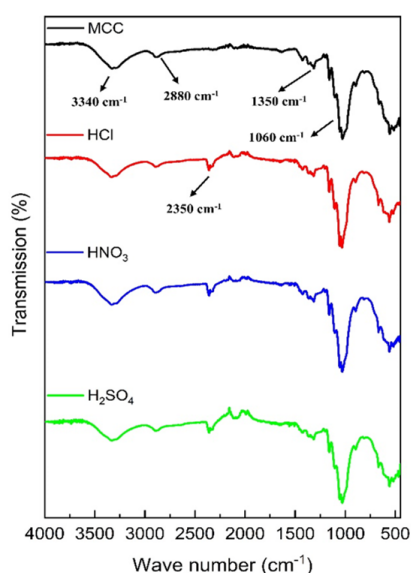


Figure 1: FTIR spectra of CNCs produced using different acids

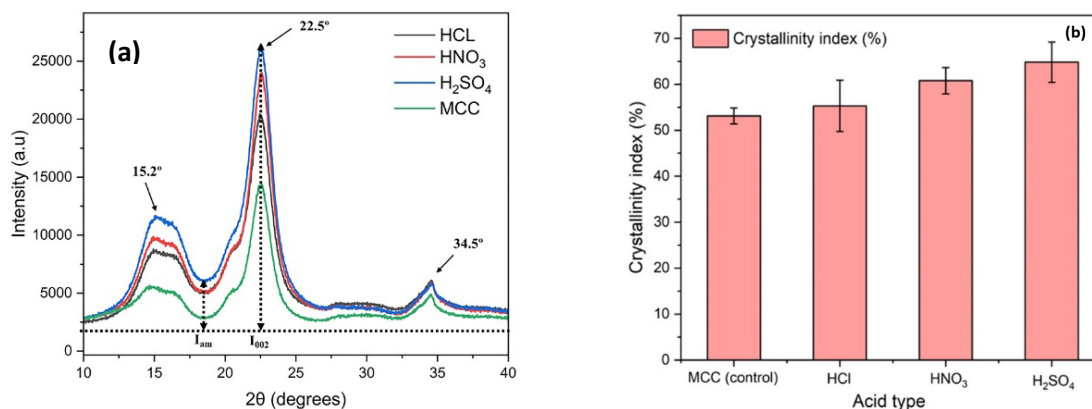


Figure 2: XRD patterns (a) and Crystallinity index % (b) of CNCs produced using different acids

On the other hand, nitric acid led to 60.7% crystallinity, which is still less than achieved with sulphuric acid. The main reason for this is the highly electro-negative atoms in the nitric acid molecule, which make it difficult to release protons. The maximum crystallinity of sulphuric acid is due to the diprotic nature, making it a more effective acid, and hence it can effectively remove the amorphous segments in the MCC, compared to nitric and hydrochloric acid.²⁰ In their study, Wang *et al.*²² used phosphotungstic acid for the conversion of wood pulp to CNCs. They studied the effect of treatment time on crystallinity, and obtained an increase of 20% in CrI. The current study also obtained a 20% increase in crystallinity, compared to the initial MCC (CrI 50%), using various acid types. Another study by Hong *et al.*³⁰ investigated the effect of various deep eutectic solvents (DES) on the CNCs, and reported maximum crystallinity (61.7%) obtained using oxalic acid solvent based treatment of MCC.

Effect of acid percentage

In previous studies, it was shown that the percentage of the acid can affect the crystallinity, as well as the surface functionalization of the CNCs.³⁰ Therefore, after selecting the acid, its content was optimized by varying the percentage of sulphuric acid as follows: 28, 30, 32, 34, and 36%.

The FTIR spectra of the obtained CNCs are presented in Figure 3. The characteristic bands of the OH and C-H stretching vibrations are noted at 3340 cm^{-1} .²⁶ The band around 1650 cm^{-1} indicates the OH vibrations due to absorbed water, that at 1350 cm^{-1} – the C-H and C-O vibrations in the polysaccharide rings of cellulose, while the band at 1060 cm^{-1} indicates the presence of C-O-C in the

pyranose ring.²⁷ The FTIR spectra of CNCs shows similar bands to those of MCC, meaning there is no chemical modification in the CNCs. However, an additional band at 2350 cm^{-1} is observed in CNCs after the acid treatment. This band reveals the presence of a thiol group due to the reaction of the hydroxyl groups of cellulose with sulphuric acid.

The XRD patterns of the CNCs (Fig. 4a) show characteristic bands at 15°, 22.5°, and 34.5°, corresponding to cellulose I, as reported previously.³¹ The calculated CrI (Fig. 4b) indicates that crystallinity increases from 58 to 64% with increasing acid percentage from 26 and 28%. This is explained by the higher efficiency in removing the amorphous regions of the higher acid concentration. However, on further increasing the acid percentage to 30% and onwards, the crystallinity decreased from 64 to 58%. The decreasing crystallinity is explained by the fact that the stronger acid starts disrupting the crystalline regions, along with the amorphous ones. Thus, at 28% acid concentration, the maximum crystallinity was obtained, and therefore this is considered the optimum acid percentage. A lower acid concentration was not efficient for removing the amorphous regions, while higher ones were too strong and destroyed the crystalline structure.³² Other studies reported close findings on the effect of acid percentage on hydrolysis results.^{33,34}

Effect of treatment time

The acid hydrolysis process of MCC was also optimized to find the most efficient duration of the treatment. Five different time periods (2, 2.5, 3, 3.5, and 4 h) were tested to select the most suitable duration for the process. The FTIR spectra of the resultant CNCs are shown in Figure 5. All the

CNCs showed the major characteristic bands around 3340, 1650, 1350, 1060 cm^{-1} , with the appearance of a new band at 2350 cm^{-1} indicating the addition of the sulphate group to CNCs.²⁸

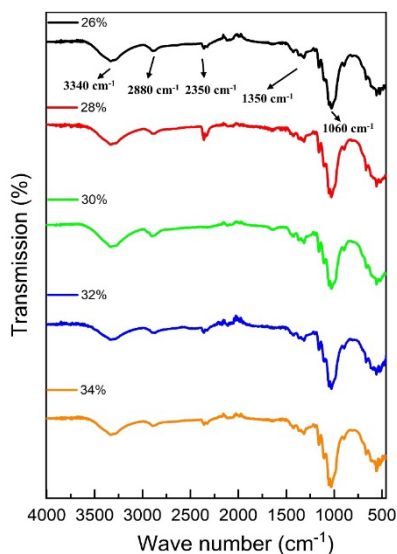


Figure 3: FTIR spectra of CNCs produced using different acid percentages

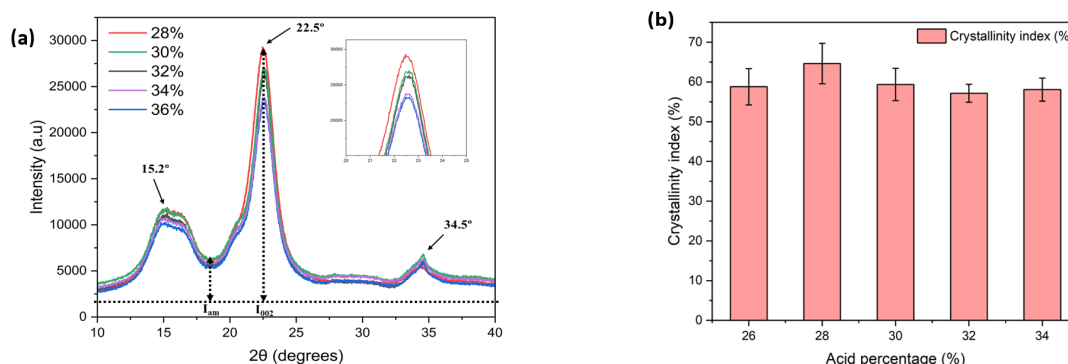


Figure 4: XRD patterns (a) and Crystallinity index % (b) of CNCs produced using different acid percentages

The XRD patterns of the obtained CNCs after treatment for different durations (Fig. 6a) reveal the characteristic bands at 15°, 22.5°, and 34.5° corresponding to cellulose I.³¹ The values of the index of crystallinity (Fig. 6b) indicate that 3.5 h of acid treatment led to the highest crystallinity of 66.2%, while the lowest duration (2 h) yielded the lowest crystallinity (61%). Overall, the crystallinity increases with an increase in treatment time from 2 h, and reaches its maximum values at 3.5 h, but decreases after this point – the treatment time of 4 h led to 61.5% crystallinity, indicating the loss of the crystalline morphology with longer treatment time. A decreasing CrI caused by longer duration of the acid treatment has also been reported in other studies.^{35,23}

Effect of treatment temperature

The temperature parameter for acid hydrolysis was also optimized using four temperature values (45, 50, 55, and 60 °C). The FTIR spectra of the CNCs obtained after treatment at these temperatures are shown in Figure 7. As may be noted, the spectra show the characteristic bands at 3340, 1650, 1350, 1060, and 2350 cm^{-1} .²⁸

The XRD patterns of the CNCs obtained at different treatment temperatures are presented in Figure 8a, showing the characteristic bands at 15°, 22.5°, and 34.5° corresponding to cellulose I.³¹ The CrI values in Figure 8b reveal that, at the temperature of 50 °C, the highest crystallinity, of 71%, was achieved. Overall, the crystallinity increases from 45 °C to 50 °C, while with further

raising the temperature, a decrease in the crystallinity was observed. The low crystallinity at low temperature indicates that it is less effective

for the removal of the amorphous regions, while at higher temperatures, it may show the disruption of the crystal regions.

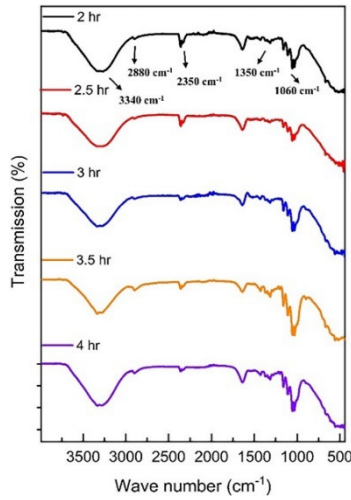


Figure 5: FTIR spectra of CNCs produced using different treatment duration

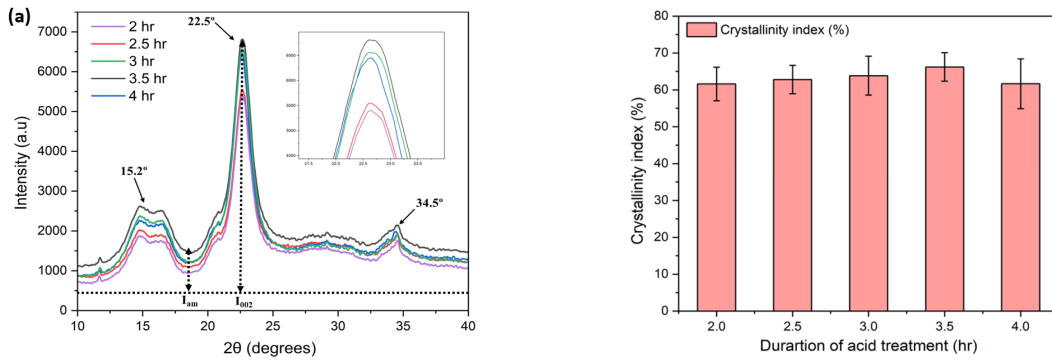


Figure 6: XRD patterns (a) and Crystallinity index % (b) of CNCs produced using different treatment duration

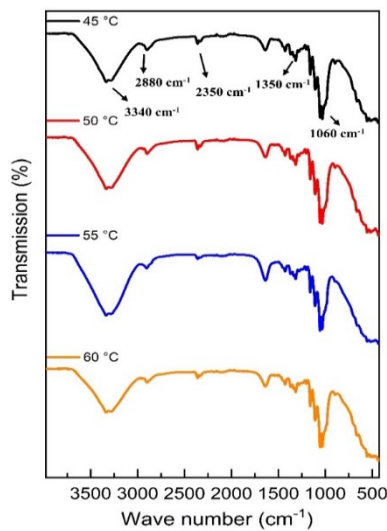


Figure 7: FTIR spectra of CNCs produced using different treatment temperatures

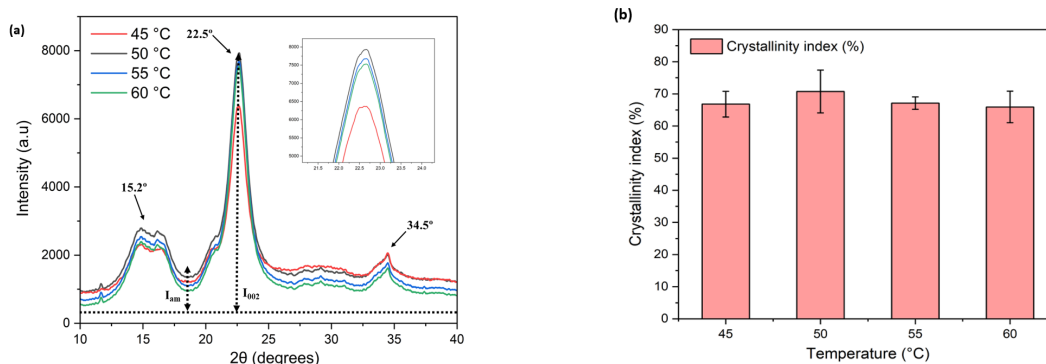


Figure 8: XRD patterns (a) and Crystallinity index % (b) of CNCs produced using different treatment temperatures

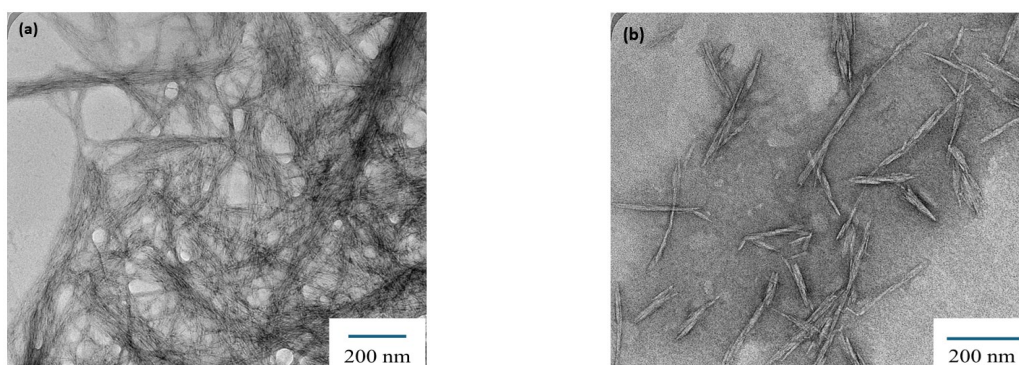


Figure 9: TEM micrographs (100 kV) of (a) microcrystalline cellulose, and (b) nanocrystalline cellulose

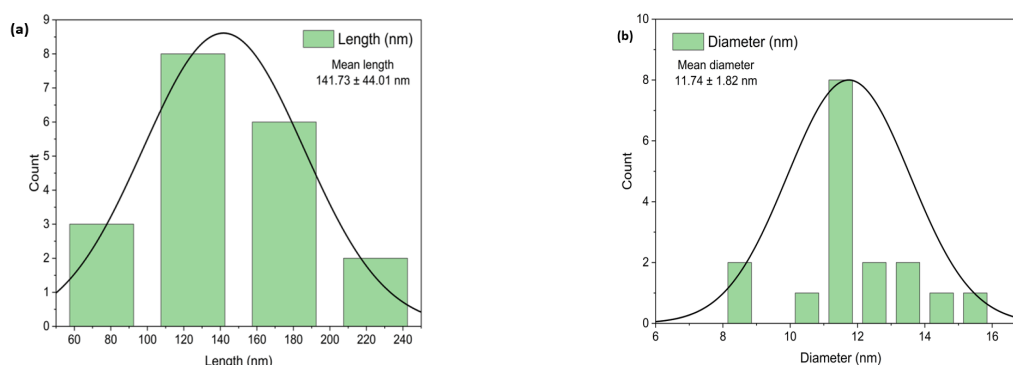


Figure 10: Particle size distribution curves for (a) length, and (b) diameter of CNCs

TEM analysis

The TEM images of the MCC and the CNCs resulting from acid hydrolysis conducted under the optimum conditions (28% H_2SO_4 acid treatment at 50 °C for 3.5 h) are shown in Figure 9. The TEM micrograph of MCC (Fig. 9a) revealed an entangled, continuous structure, without disruptions. The structure is composed of crystalline and amorphous regions. Amorphous regions are not considered suitable for the drug delivery application, especially for achieving sustained drug release, as random arrangement of atoms can result in variable drug loading and burst release.^{36,37} The acid hydrolysis removes the

amorphous regions from MCC and results in a highly crystalline structure of CNCs (CrI 70%) (Fig. 9b).³⁸

The particle size distribution of the CNCs obtained under the optimized conditions is shown in Figure 10. The length distribution curve reveals a mean length of 141.73 nm, while the mean diameter was 11.74 nm. The aspect ratio obtained is thus much lower than that of previous studies, being around 12.07.²³ Cherian *et al.*³⁹ reported higher crystallinity – of 81.54% –, but the aspect ratio was 17.8. A lower aspect ratio is highly suitable for biomedical applications, as it improves cellular uptake and lowers the cytotoxicity. Thus,

the current study was successful in obtaining CNCs with high crystallinity and low aspect ratio, which could find application in the biomedical sector.⁴⁰

CONCLUSION

The current study optimized the parameters of the acid hydrolysis process in order to achieve CNCs from microcrystalline cellulose with higher crystallinity and lower aspect ratio, which could be suitable for biomedical applications. The optimization results were then verified by the XRD and FTIR analyses of the obtained CNCs. Acid hydrolysis of microcrystalline cellulose at 28% of H₂SO₄ treatment at 50 °C for 3.5 h yielded the highest percentage of crystallinity. TEM analysis was then used to determine the dimensions of the CNCs obtained under optimum parameters, and it revealed a mean length of 141.73 nm and a diameter of 11.74 nm, with an aspect ratio of 12.07. The findings of this work can be useful at a lab or industrial scale to develop CNCs, with improved crystallinity and low aspect ratio for biomedical applications.

ACKNOWLEDGEMENTS: The authors would like to thank Universiti Malaysia Pahang Al-Sultan Abdullah for the Distinguished Research Grant (University Reference RDU243002).

REFERENCES

- 1 Y. Liu, S. Ahmed, D. E. Sameen, Y. Wang, R. Lu *et al.*, *Trends Food Sci. Technol.*, **112**, 532 (2021), <https://doi.org/10.1016/j.tifs.2021.04.016>
- 2 M. H. Syed, M. A. K. M. Zahari, M. M. R. Khan, M. D. H. Beg and N. Abdullah, *J. Drug Deliv. Sci. Technol.*, **80**, 104121 (2023), <https://doi.org/10.1016/j.jddst.2022.104121>
- 3 H. Seddiqi, E. Olliaei, H. Honarkar, J. Jin, L. C. Geonzon *et al.*, *Cellulose*, **28**, 1893 (2021), <https://doi.org/10.1007/s10570-020-03674-w>
- 4 M. H. Syed, M. M. R. Khan, M. A. K. M. Zahari, M. D. H. Beg and N. Abdullah, *Eur. Polym. J.*, **197**, 112352 (2023), <https://doi.org/10.1016/j.eurpolymj.2023.112352>
- 5 M. H. Syed, M. M. R. Khan, M. A. K. M. Zahari, M. D. H. Beg and N. Abdullah, *Int. J. Biol. Macromol.*, **253**, 126735 (2023), <https://doi.org/10.1016/j.ijbiomac.2023.126735>
- 6 C. Verma, V. Singh and A. AlFantazi, *Phys. Chem. Chem. Phys.*, **26**, 11217 (2024), <https://doi.org/10.1039/D3CP06057H>
- 7 M. H. Syed, S. Qutaba, M. A. K. M. Zahari, N. Abdullah, M. Shoaib *et al.*, *Egypt. J. Chem.*, **66**, 255 (2023), <https://doi.org/10.21608/EJCHEM.2022.148407.6418>

- 8 S. Sumaiyah, P. A. Z. Hasibuan, H. Syahputra and M. F. Lubis, *J. Appl. Pharm. Sci.*, **14**, 165 (2024), <https://dx.doi.org/10.7324/JAPS.2024.179096>
- 9 M. H. Syed, S. Qutaba, L. Syed, M. A. K. M. Zahari, N. Abdullah *et al.*, *Surf. Innov.*, **12**, 30 (2024), <https://doi.org/10.1680/jsuin.22.01073>
- 10 L. K. Kian, M. Jawaid, H. Ariffin and Z. Karim, *Int. J. Biol. Macromol.*, **114**, 54 (2018), <https://doi.org/10.1016/j.ijbiomac.2018.03.065>
- 11 H. Yan, X. Chen, H. Song, J. Li, Y. Feng *et al.*, *Food Hydrocoll.*, **72**, 127 (2017), <https://doi.org/10.1016/j.foodhyd.2017.05.044>
- 12 J. T. Orasugh, N. R. Saha, G. Sarkar, D. Rana, D. Mondal *et al.*, *Int. J. Biol. Macromol.*, **109**, 1246 (2018), <https://doi.org/10.1016/j.ijbiomac.2017.11.123>
- 13 B. Li, W. Xu, D. Kronlund, J.-E. Eriksson, A. Maattanen *et al.*, *Paper Biomater.*, **3**, 35 (2018), <https://doi.org/10.26599/PBM.2018.9260026>
- 14 W. Kargupta, R. Seifert, M. Martinez, J. Olson, J. Tanner *et al.*, *Ind. Crop. Prod.*, **171**, 113868 (2021), <https://doi.org/10.1016/j.indcrop.2021.113868>
- 15 H. Yousefian and D. Rodrigue, *Polym. Compos.*, **37**, 1473 (2016), <https://doi.org/10.1002/pc.23316>
- 16 V. Landry, A. Alemdar and P. Blanchet, *For. Prod. J.*, **61**, 104 (2011), <https://doi.org/10.13073/0015-7473-61.2.104>
- 17 M. H. Syed, S. A. Rubab, S. R. Abbas, S. Qutaba, M. A. K. Mohd Zahari *et al.*, *J. Biochem. Mol. Toxicol.*, **37**, e23382 (2023), <https://doi.org/10.1002/jbt.23382>
- 18 S. Mishra, P. S. Kharkar and A. M. Pethe, *Carbohydr. Polym.*, **207**, 418 (2019), <https://doi.org/10.1016/j.carbpol.2018.12.004>
- 19 M. H. Syed, M. M. R. Khan, M. A. K. M. Zahari, M. D. H. Beg and N. Abdullah, *Green Mater.*, **13**, 396 (2025), <https://doi.org/10.1680/jgrma.24.00057>
- 20 A. Q. Almashhadani, C. P. Leh, S.-Y. Chan, C. Y. Lee and C. F. Goh, *Carbohydr. Polym.*, **286**, 119285 (2022), <https://doi.org/10.1016/j.carbpol.2022.119285>
- 21 M. H. Syed, M. M. R. Khan, M. A. K. M. Zahari, M. D. H. Beg and N. Abdullah, *J. Appl. Polym. Sci.*, **141**, e56291 (2024), <https://doi.org/10.1002/app.56291>
- 22 Y. Liu, H. Wang, G. Yu, Q. Yu, B. Li *et al.*, *Carbohydr. Polym.*, **110**, 415 (2014), <https://doi.org/10.1016/j.carbpol.2014.04.040>
- 23 A. Hachaichi, B. Kouini, L. K. Kian, M. Asim, H. Fouad *et al.*, *Materials*, **14**, 5313 (2021), <https://doi.org/10.3390/ma14185313>
- 24 Z. A. Zianor Azrina, M. D. H. Beg, M. Y. Rosli, R. Ramli, N. Junadi *et al.*, *Carbohydr. Polym.*, **162**, 115 (2017), <https://doi.org/10.1016/j.carbpol.2017.01.035>
- 25 A. Budiman, A. L. Handini, M. N. Muslimah, N. V. Nurani, E. Laelasari *et al.*, *Polymers*, **15**, 3380 (2023), <https://doi.org/10.3390/polym15163380>
- 26 S. Rezanezhad, N. Nazarnezhad, H. Resalati and S. M. Zabihzadeh, *BioResources*, **17**, (2022), <https://doi.org/10.15376/biores.17.3.4607-4622>
- 27 W. Wulandari, A. Rochliadi and I. Arcana, *IOP Conf. Ser.: Mater. Sci. Eng.*, **107**, 012045 (2016)

- ²⁸ F. Beltramino, M. B. Roncero, A. L. Torres, T. Vidal and C. Valls, *Cellulose*, **23**, 1777 (2016), <https://doi.org/10.1007/s10570-016-0897-y>
- ²⁹ Q. Chen, Y. Shi, G. Chen and M. Cai, *Int. J. Biol. Macromol.*, **142**, 846 (2020), <https://doi.org/10.1016/j.ijbiomac.2019.10.024>
- ³⁰ F. Wu, W. He, H. Hong and T. Wei, *Cellulose Chem. Technol.*, **58**, 959 (2024), <https://doi.org/10.35812/CelluloseChemTechnol.2024.58.83>
- ³¹ M. M. El-Sheekh, W. E. Yousuf, E.-R. Kenawy and T. M. Mohamed, *Sci. Rep.*, **13**, 10188 (2023), <https://doi.org/10.1038/s41598-023-37287-7>
- ³² D. Sartika, K. Syamsu, E. Warsiki and F. Fahma, *IOP Conf. Ser.: Earth Environ. Sci.*, **355**, 012109 (2019), <https://doi.org/10.1088/1755-1315/355/1/012109>
- ³³ N. Pandi, S. H. Sonawane and K. Anand Kishore, *Ultrason. Sonochem.*, **70**, 105353 (2021), <https://doi.org/10.1016/j.ultsonch.2020.105353>
- ³⁴ J.-Y. Yang, Q.-F. Yu and M.-F. Li, *Bioresour. Technol.*, **384**, 129365 (2023)
- ³⁵ N. Fitriani, A. S. Aprilia and N. Arahman, *IOP Conf. Ser.: Mater. Sci. Eng.*, **796**, 012007 (2020), <https://doi.org/10.1088/1757-899X/796/1/012007>
- ³⁶ S. Puhl, L. Meinel and O. Germershaus, *Asian J. Pharm. Sci.*, **11**, 469 (2016), <https://doi.org/10.1016/j.ajps.2016.06.003>
- ³⁷ J. Zhang, M. Guo, M. Luo and T. Cai, *Asian J. Pharm. Sci.*, **18**, 100834 (2023), <https://doi.org/10.1016/j.ajps.2023.100834>
- ³⁸ C. Danumah and H. Fenniri, *MRS Online Proc. Libr.*, **1312**, 525 (2011), <https://doi.org/10.1557/opl.2011.132>
- ³⁹ R. M. Cherian, R. T. Varghese, T. Antony, A. Malhotra, H. Kargarzadeh *et al.*, *Int. J. Biol. Macromol.*, **253**, 126571 (2023)
- ⁴⁰ A. M. Weiss, N. Macke, Y. Zhang, C. Calvino, A. P. Esser-Kahn *et al.*, *ACS Biomater. Sci. Eng.*, **7**, 1450 (2021), <https://doi.org/10.1021/acsbiomaterials.0c01618>